Catalysis Today 158 (2010) 162–169

Contents lists available at ScienceDirect

Catalysis Today

journal homepage: www.elsevier.com/locate/cattod

Mo–W-containing tetragonal tungsten bronzes through isomorphic substitution of molybdenum by tungsten

Pablo Botella [a], Benjamín Solsona [a,b], José M. López Nieto [a,*], Patricia Concepción [a], Jose L. Jordá [a], María Teresa Doménech-Carbó [c]

[a] Instituto de Tecnología Química (UPV-CSIC), Campus Universidad Politécnica de Valencia, Avda. de los Naranjos s/n, 46022 Valencia, Spain
[b] Departamento de Ingeniería Química, Universidad de Valencia, 46100 Burjassot, Spain
[c] Instituto de Restauración del Patrimonio, Universidad Politécnica de Valencia, 46022 Valencia, Spain

ARTICLE INFO

Article history:
Available online 29 June 2010

Keywords:
Mo–V–Te–Nb–W–P–O mixed metal oxides
Hydrothermal synthesis
Isomorphic substitution of molybdenum by tungsten
TTB-bronze
Partial oxidation of propene

ABSTRACT

Mixed metal oxides based in Mo(W)–Nb–V–Te with tetragonal tungsten bronze (TTB) structure have been synthesized by a hydrothermal method from aqueous solutions of the corresponding Keggin-type heteropolyacids and further heat-treatment in N_2 at 700 °C. The materials have been characterized by several physico-chemical techniques, i.e. XRD, Raman, FTIR, SEM-EDS, and TEM. This procedure allows controlling the chemical species to be distributed in the different interstices of the TTB skeleton, which is a key factor to regulate the catalytic properties of the final solid. In this sense, the isomorphic replacement of Mo by W results in lattice parameter and crystal morphology variation, although the TTB structure is preserved to different degrees of substitution. The incorporation of tellurium to the TTB framework leads to active and selective catalysts in the partial oxidation of propene to acrolein.

1. Introduction

Tetragonal tungsten bronze (TTB)-type oxides compose a large and extensively studied family of materials with a wide variety of cations. Although the term "tetragonal tungsten bronze" was formerly introduced for the non-stoichiometric compound K_xWO_3 (x = 0.4–0.6) [1], it was further extended to other compounds with a similar structure and different transition metals as central atom.

Standard methods for preparation of Mo- or W-containing bronzes involve the reaction of the component materials in the solid state at high temperatures [2], or the thermal degradation of polyoxometallates [3–6]. Conversely, soft chemical methods often allow producing new materials that cannot be synthesized by using solid state reactions at high temperature. The production of highly uniform materials requires precursors containing the appropriate components dispersed at molecular level with the desired stoichiometry. Here, hydrothermal synthesis has been proposed as an interesting alternative to prepare mixed metal oxides [7–9]. In this synthesis, the use of polyoxometallates as precursors is widely extended, although most of the examples concern applications of Anderson-type oxoanions. Very recently our group has presented the synthesis of Mo-containing TTB derived from the Nb_2O_5/WO_3 system by heat-treatment of amorphous precursors hydrothermally synthesized from aqueous solutions of Keggin-type heteropolyacids together with vanadium and niobium salts [10–12]. These materials have found application as active and very selective catalysts for the partial oxidation of short-chain olefins when incorporating in the framework an element of the V and VI groups, but especially tellurium [11]. In addition, the tetragonal bronzes display a catalytic behavior similar to that observed for the pseudohexagonal bronze (the so-called M2-phase) although some of them are more active for propene oxidation [10]. However, tuning of the composition of this TTB phase is of interest not only as a candidate for olefin oxidation, but also as a possible component of an active and selective alkane oxidation catalytic system.

In the present work we describe a synthesis method for the preparation of Mo–W–Nb–V–P–Te mixed oxides with TTB structure where molybdenum is partially or fully replaced by tungsten through isomorphic substitution. Structural parameters are tuned in order to achieve homogeneous dispersion of MO_6 octahedra (M = Mo,W) in the TTB framework. These materials find application as selective catalysts in the partial oxidation of propene to acrolein and acrylic acid. Improved catalytic performance is explained on the basis of the isolation of Mo-sites and the synergetic effect between Mo- and W-centers.

* Corresponding author. Tel.: +34 96 387 7808; fax: +34 96 387 7809.
E-mail address: jmlopez@itq.upv.es (J.M. López Nieto).

0920-5861/$ – see front matter © 2010 Elsevier B.V. All rights reserved.
doi:10.1016/j.cattod.2010.05.024

2. Experimental

2.1. Synthesis of TTB-bronzes

Materials have been prepared by hydrothermal synthesis from gels containing $H_3PMo_{12}O_{40}$ and/or $H_3PW_{12}O_{40}$ (Aldrich), vanadyl sulfate (Aldrich) niobium oxalate (CBMM) and telluric acid (Aldrich) [12]. The resulting gels, with a concentration of 3.3 mmol of heteropolyacid in 40 ml of H_2O and a Mo(W)/Nb/V/P/Te atomic ratio of $x(y)$/0.17/0.20/0.08/0.04 (where $x+y=1$), were introduced in a Teflon-lined, stainless steel autoclave and heated at 175 °C for 48 h. The solid so obtained was filtered off, washed (with 0.2 l/g of distilled water) and dried at 80 °C for 16 h. Finally, the samples were heated (3 °C/min of heating rate) at 700 °C in flowing N_2 for 2 h and (then cooled with a cooling rate of 5 °C/min). Materials were named as MW*n*, where *n* is related to the W/(Mo + W) atomic ratio in the synthesis gel (i.e., MW45 corresponds to a sample with a W/(Mo + W) atomic ratio of 0.45).

2.2. Characterization of TTB-bronzes

Average chemical composition of both as-prepared and heat-treated samples was determined by inductively couple plasma (ICP).

The surface areas were measured on a Micromeritics ASAP 2000 instrument by adsorption of krypton.

X-ray powder diffraction (XRD) measurements were performed in a PANalytical X'Pert PRO diffractometer using Cu Kα1,2 radiation and an X'Celerator detector in Bragg-Brentano geometry. The crystalline phases were identified by matching experimental patterns to the JCDS powder diffraction file (reference number 80-02136) of the TTB $Ba_3Nb_5O_{15}$. Unit cell parameters were refined using the program FullProf [13].

Samples for transmission electron microscopy (TEM) were ultrasonically dispersed in 2-propanol and transferred to carbon coated copper grids. TEM micrographs were collected in a Philips CM-10 microscope operating at 100 kV.

Scanning electron microscopy (SEM) micrographs were collected in a JEOL 6300 microscope operating at 20 kV, 2×10^{-9} A beam current and 15 mm as working distance. Samples were carbon coated to eliminate charging effects. The quantitative EDS analysis was performed using an Oxford LINK ISIS System with the SEMQUANT program, which introduces the ZAF correction. The counting time was 100 s for major and minor elements.

Infrared spectra of KBr wavers were recorded at room temperature in the 300–3900 cm^{-1} region with a Nicolet 205xB spectrophotometer, equipped with a Data Station, at a spectral resolution of 1 cm^{-1} and accumulations of 128 scans.

Raman spectra were obtained with an "in via" Renishaw spectrometer, equipped with an Olympus microscope. The 514 nm line of an Ar^+-ion laser (Spectra Physics) was used for excitation, with a power of 1.25 mW on the sample. The spectra were recorded at 10 s exposure time and 20 accumulations. The spot size was 0.5 μm and an average of three sampling spots was collected for each sample.

2.3. Catalytic tests

Catalytic tests in propylene oxidation have been undertaken at atmospheric pressure using a fixed-bed quartz tubular flow reactor (i.d. 10 mm; length 300 mm) which has been heated electrically. The reactor is equipped with a coaxial thermocouple for temperature profiling. Reaction temperatures from 340 to 420 °C have been studied. The feed was fixed to give a $C_3H_6/O_2/He/H_2O$ molar ratio of 1.5/6.0/77.5/15, meanwhile the catalyst weight (from 0.1 to 1.5 g) and the total flow (from 25 to 50 ml min^{-1}) were varied in order to obtain different conversions at a given reaction temperature. Typical experiments were conducted using 1 g of catalyst and a total flow of 50 ml/min, leading to a GHSV of 3000 h^{-1} (without considering the volume of the silicon carbide). Catalyst samples (particle size between 0.3 and 0.5 mm) were introduced in the reactor diluted with Norton Silicon Carbide (0.5–0.75 mm particle size) in order to keep a constant volume (2 cm^3) in the catalytic bed and quench thermal effects derived from the exothermic nature of the reaction. Reactants and reaction products were analyzed online by gas chromatography using two different columns: Molecular Sieve 5A and Porapak Q [9]. Blank runs showed that under the experimental conditions used in this work the homogeneous reaction could be neglected.

3. Results and discussion

3.1. Structural characterization

After the heat-treatment in N_2 these materials show metallic sheen and changing color depending on the composition: from purple for W-free sample (MW0) to dark brown for Mo-free mixed oxide (MW100). In all cases, solids with low surface area (below 10 $m^2\ g^{-1}$) were obtained. A summary of the most important physical and chemical characteristics of these materials is presented in Table 1.

Chemical composition of heat-treated materials matches reasonably well with synthesis gel composition, although molybdenum is incorporated to a greater extent than tungsten. Furthermore, the crystal by crystal EDS microanalysis shows a homogenous distribution of both elements in every analyzed spot (see Table 1).

Powder XRD reports of heat-treated materials are presented in Fig. 1 (as-synthesized samples showed in all cases the same non-crystalline pattern). Diffraction maxima match with those of a basic TTB structure (JCPDS file no. 80-02136), although the relative intensities are closer to those reflections of the ordered $M_{17}O_{47}$ phase [12]. W-free sample (MW0, Fig. 1a) presents main peaks at $2\theta = 22.2$, 23.3, 26.6, 30.5, 33.2 and 35.0°. No significant reflection is visible in the low angle zone (<12°), indicating that certain extra order in respect to the TTB must occur but only to a low extent. Other minor phases are not detected in these materials. According to previous results, these materials are structural analogues of the binary system Nb_2O_5/WO_3 [12]. In a standard configuration, this system presents linked MO_6 octahedra to give five-membered rings arranged around square tunnels and MO_7 polyhedra that share the equatorial edges with five octahedra. A certain portion of the pentagonal tunnels are filled with metal-oxygen chains (preferentially by niobium atoms), thus, leading to a pentagonal bipyramidal coordination of the corresponding metal cation [14,15]. Strings of these units connected along the perpendicular direction forms the so-called pentagonal columns (PCs).

The replacement of Mo by W in the framework results in a shift of the peak positions due to unit cell changes (Fig. 1). The isomorphic substitution of W for Mo is possible considering the respective ionic radius and coordination. The Shannon ionic radius for 6-coordinated Mo^{6+} and W^{6+} is 0.73 and 0.74 Å, respectively [16]. Such a proximity in size agrees well with the fact that all Mo can be replaced by W. In this case, due to the slightly larger ionic radius of tungsten the lattice parameters change when increasing its content, i.e., the *a*-axis increases and the *c*-axes decreases (Fig. 2). Both lattice parameters vary linearly with the degree of substitution for ratios $W/(W+Mo) \geq 0.33$, thus, following Vegard's law [17], as already observed when replacing Mo by W in other Mo-containing bronzes [18,19]. This confirms an homogeneous distribution of both cations in the crystalline network. Concerning the unit cell volume (Fig. 2c), as the replacement of Mo by W leads to opposite actions,

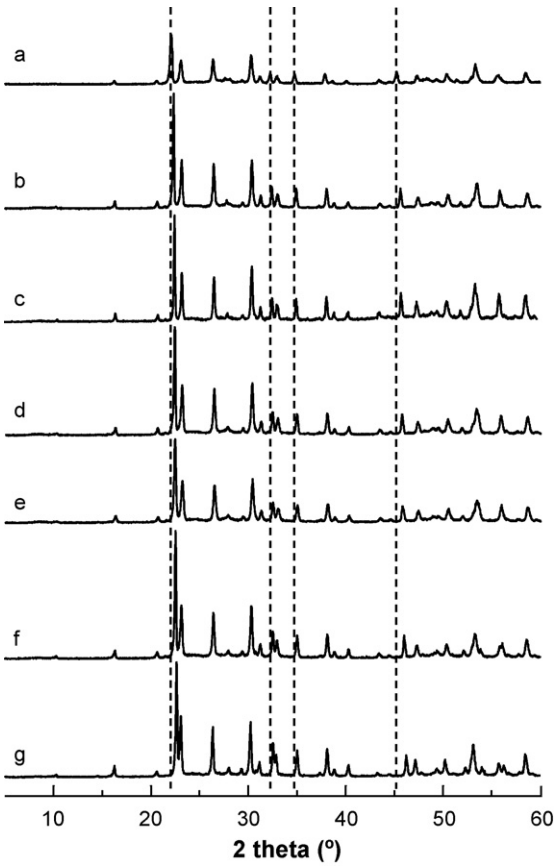

Fig. 1. (a) X-ray diffraction patterns of Mo–W-based mixed oxides with TTB structure (N_2/700 °C): (a) MW0; (b) MW25; (c) MW40; (d) MW45; (e) MW50; (f) MW75; (g) MW100. Dashed vertical lines indicate the position of some peaks of MW0 as a reference of the shift of peak positions with the replacement of Mo by W, due to unit cell changes. Chemical compositions are shown in Table 1.

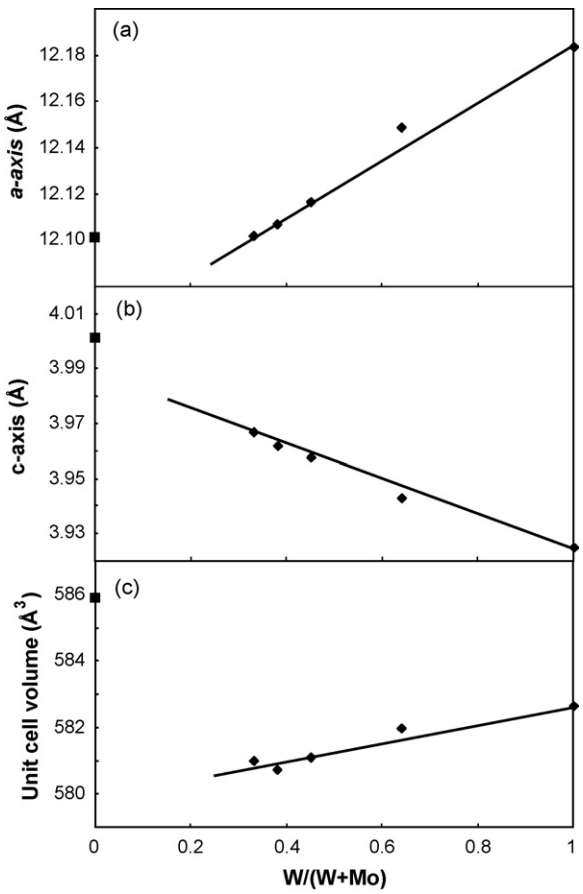

Fig. 2. Variation of unit cell parameters in the TTB structure as a function of the degree of substitution of Mo by W: (a) *a*-axis; (b) *c*-axis; (c) unit cell volume.

expansion of the *ab*-plane and contraction of the *c*-axis, the evolution of the unit cell volume is not easy to predict. In this case, we have found that for ratios W/(W + Mo) ≥ 0.33 the substitution of Mo by W results in an increase of the unit cell volume, which is in good agreement with the fact that W ion is somewhat larger than the Mo ion.

Nevertheless, the lattice parameters of the W-free sample (MW0) do not fit to the linear distribution of the W-containing materials. In this case, it should be taken into account the possible contribution of other elements, particularly of niobium, to the skeleton formation of the TTB phase. Here, recent studies of our group by high resolution electron microscopy (HREM) and selected area electron diffraction (SAED) have provided a clear correspondence between the structural features observed in the reciprocal lattice of the Mo–Nb–V-containing TTB-type oxide and those of the system Nb_2O_5/WO_3 [12]. This has been described as a disordered distribution of filled PC in a well-ordered basic TTB framework made of molybdenum, niobium and vanadium. It is assumed that vanadium and niobium atoms are placed in the MO_6 octahedra, although niobium can also be filling partially the PC. While the incorporation of 6-coordinated V^{4+} (ionic radius = 0.72 Å) has no effect on the lattice parameters, 6-coordinated Nb^{5+} (0.78 Å) is clearly larger than Mo^{6+} and can modify the unit cell of the TTB structure. On the other hand, the observed enlargement of the *ab*-plane for W-containing materials appears to be sufficient to accommodate Nb^{5+} in the framework, even for high niobium loadings (i.e., sample MW100).

In the case of tellurium, it has been found experimental evidence of its partial inclusion in the tunnels of the TTB structure, as

Table 1
Compositional and textural characteristics of Mo–W-based mixed oxides with TTB structure.

Sample	W/(W + Mo)[a]	Area BET ($m^2\ g^{-1}$)	Metal atomic ratio	
			Bulk[b]	Crystal by crystal[c]
MW0	0.00	2.0	$Mo_1Nb_{0.56}V_{0.17}P_{0.10}Te_{0.15}$	$Mo_1Nb_{0.38}V_{0.24}P_{0.03}Te_{0.08}$
MW25	0.25	5.0	$Mo_{0.70}W_{0.30}Nb_{0.41}V_{0.20}P_{0.08}Te_{0.03}$	$Mo_{0.72}W_{0.28}Nb_{0.39}V_{0.18}P_{0.08}Te_{0.03}$
MW40	0.40	4.5	$Mo_{0.68}W_{0.32}Nb_{0.40}V_{0.22}P_{0.07}Te_{0.04}$	$Mo_{0.64}W_{0.36}Nb_{0.43}V_{0.21}P_{0.07}Te_{0.04}$
MW45	0.45	6.8	$Mo_{0.62}W_{0.38}Nb_{0.42}V_{0.21}P_{0.09}Te_{0.0.04}$	$Mo_{0.63}W_{0.37}Nb_{0.43}V_{0.35}P_{0.06}Te_{0.05}$
MW50	0.50	6.8	$Mo_{0.55}W_{0.45}Nb_{0.63}V_{0.18}P_{0.06}Te_{0.06}$	$Mo_{0.54}W_{0.46}Nb_{0.41}V_{0.20}P_{0.08}Te_{0.06}$
MW75	0.75	7.7	$Mo_{0.36}W_{0.64}Nb_{0.53}V_{0.24}P_{0.12}Te_{0.07}$	$Mo_{0.48}W_{0.52}Nb_{0.55}V_{0.23}P_{0.16}Te_{0.04}$
MW100	1.00	9.5	$W_1Nb_{0.69}V_{0.25}P_{0.05}Te_{0.23}$	$W_1Nb_{0.86}V_{0.29}P_{0.06}Te_{0.13}$

[a] W/(W + Mo) atomic ratio in the synthesis gel (Mo,W = 0–1, Mo + W = 1).
[b] Atomic composition as determined by ICP analysis.
[c] Average atomic composition as determined by microanalysis EDS of several crystallites.

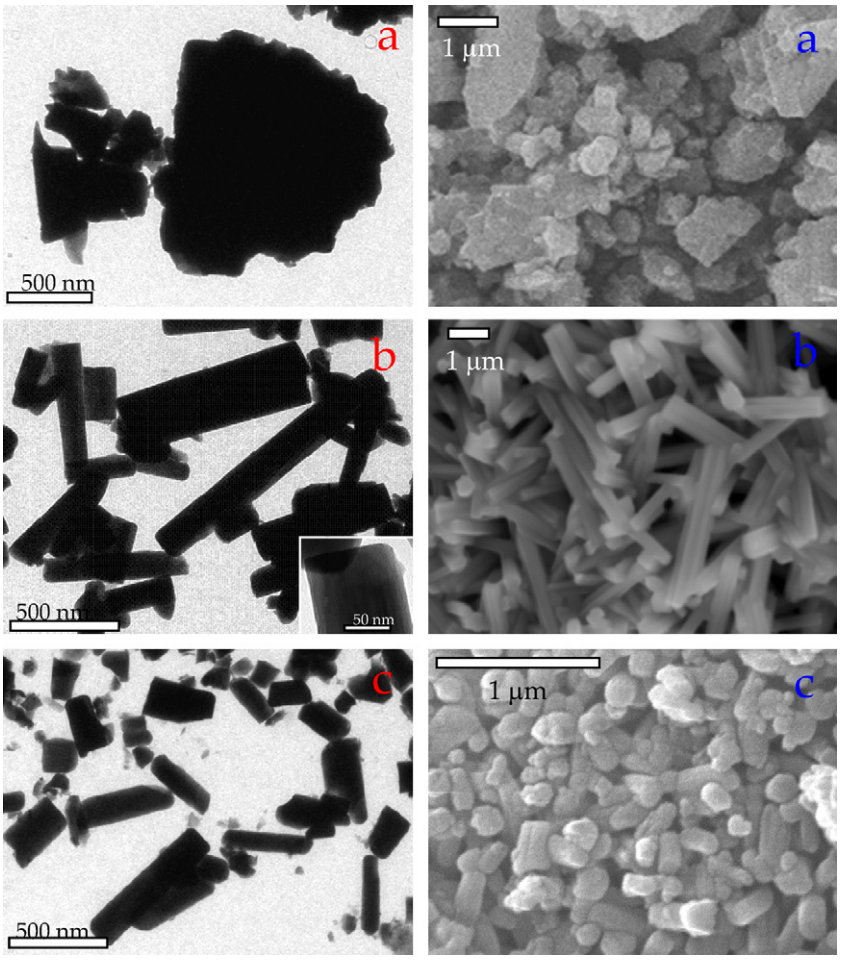

Fig. 3. TEM (left) and secondary electron (right) images of Mo–W-based mixed oxides with TTB structure: (a) MW0; (b) MW50; (c) MW100. The inset in image (b) corresponds to the high magnification of a crystal of the MW50 sample.

the niobium does not fill completely the PC [12]. Although a complete incorporation of this element in the framework is still to be confirmed, no sign of the lattice parameters becoming constant or growing diffuse features in the background of the XRD patterns is observed with increasing substitution, thus, supporting the idea that, at least for this range of compositions, the formation of an amorphous bulk phase can be ruled out.

Crystal morphology and size of heat-treated materials with different W/(Mo + W) atomic ratios has been studied by TEM and SEM (Fig. 3) and the local chemical composition was determined in the scanning electron microscope by means of EDS analysis of individual crystals (Table 1). Besides some polydispersity due to strong sintering during the thermal treatment, the incorporation of tungsten leads to smaller crystallite sizes, with an average particle diameter one order of magnitude lower in the case of Mo-free sample. In this sense, the average diameter, as determined from TEM images by measuring at least 100 particles, is (mean ± standard deviation) 1283 ± 556 nm for the W-free sample (MW0), 480 ± 260 nm for MW50 sample, and 388 ± 147 nm for the Mo-free material (MW100). Thus, since no internal porosity can be considered in these solid, it can be concluded that the partial substitution of Mo by W favors an increase in the number of accessible active sites. EDS analysis shows an homogeneous distribution of both Mo and W in all crystals. However, when increasing the W-content the observed atomic ratio W/(W + Mo) in the heat-treated materials is somewhat lower than that in the synthesis gel (about 80% of the maximum). In this sense, we think the superior ionic ratio of W versus Mo limits its incorporation to the TTB structure. On the other hand, vanadium, niobium and tellurium appear homogenously distributed in the different crystallites.

Infrared and Raman spectra of heat-treated materials are presented in Fig. 4. The infrared spectra of W-free sample (MW0) shows a shoulder at 987 cm^{-1}, and broad bands at 881, 750, 642 and 543 cm^{-1}, in addition to a shoulder at 445 cm^{-1} (Fig. 4A, spectrum a). According to previous results [12,19] the high frequency signal is assigned to isolated oxo-molybdenum species, i.e., terminal Mo=O double bond stretching vibrations, while the low frequency bands at 642, 543 and 445 cm^{-1} are related to Mo–O–Y (Y = Mo, V, Nb) bridge vibrations, and the band at 750 cm^{-1} is due to the symmetric vibration of Nb–O–Mo bond. The appearance of broad bands is related to an important heterogeneity in Mo–O–Y bridges in Mo-based bronzes [20,21], together with some contribution of IR bands associated with PO_2 bending vibrations at 512–540 cm^{-1} [22] (Fig. 4).

Partial or total substitution of Mo by W in the crystalline framework (samples MW25 to MW100) produces a shift of several bands to lower frequencies (Fig. 4A, spectra b–f). In particular, both IR bands at 881 and 750 cm^{-1} associated with Mo–O–Mo and Nb–O–Mo stretching vibration respectively, shift to lower frequencies, 852 and 742 cm^{-1} (W–O–W and W–O–Nb stretching vibration, respectively). On the other hand, a band at 965 cm^{-1} starts to appear in the W-rich samples, which could be related to a W monooxo species [23]. However, we must indicate that the in plane PO_2 symmetrical stretching vibration is also characterized by an IR band at 967 cm^{-1} [24], and thus its contribution cannot be completely ruled out. Conversely, no significant change is detected

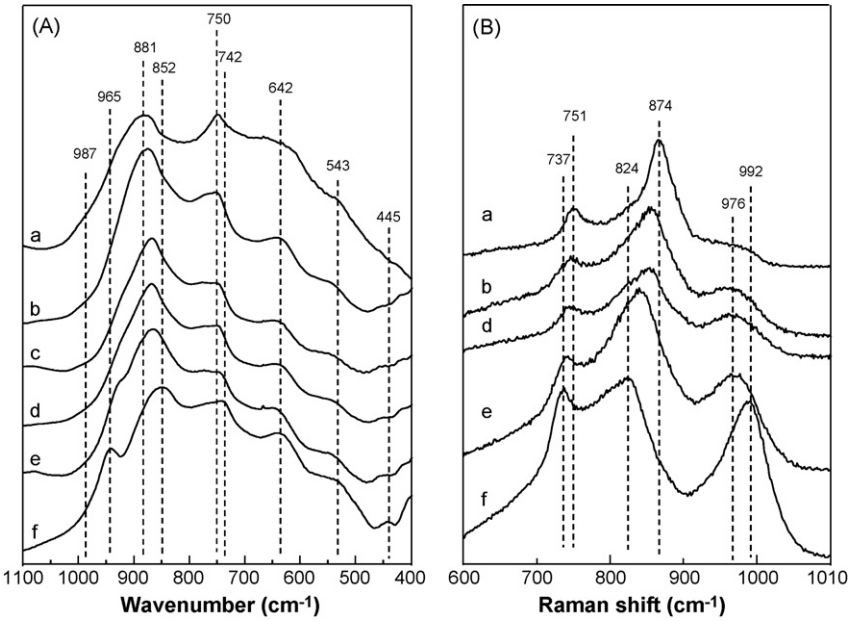

Fig. 4. FTIR (A) and Raman (B) spectra of Mo–W-based mixed oxides with TTB structure: (a) MW0; (b) MW25; (c) MW40; (d) MW50; (e) MW75; (f) MW100.

in the 400–700 cm^{-1} region, therefore, suggesting that the average crystalline structure is not modified by the incorporation of tungsten. Also, the presence of tellurium in the framework does not change the structural parameters of the TTB [12].

Raman spectra of selected materials with different W/(W + Mo) molar ratios are presented in Fig. 4B. W-free sample (MW0) shows a broad and weak band at 976 cm^{-1} assigned to vibrations of Mo=O double bonds and two intense bands at 874 and 751 cm^{-1} due to vibrations of Mo–O–Mo bridges (Fig. 4B, spectrum a) [25]. Partial substitution of Mo by W shifts the last two bands to lower frequencies, 824 and 737 cm^{-1} for W–O–W and Nb–O–W bridges [26,27], respectively, in addition to the appearance of a new band at 992 due to W=O [23] or V=O [28] species. The shift of the bands and the appearance of new bands corresponding to Mo- or W-free materials, depending on the W/(W + Mo) atomic ratio, suggests an homogeneous substitution of W by Mo along the crystalline structure.

XPS characterization of W free, Mo free and Mo–W-containing bronze samples (i.e. MW50 and MW75) has been performed in order to determine the surface composition and the oxidation state of each element present in representative catalysts. The XPS results are shown in Table 2. The surface composition differs somewhat from their bulk composition in the way that an enrichment of tellurium is observed on the catalysts surface of all samples. In addition, the Nb/(W + Mo) and V/(W + Mo) surface atomic ratios increase when increasing the W-content of catalysts, suggesting that W^{6+} can facilitate the incorporation of both elements more easily than in the case of Mo-containing materials.

On the other hand, while Mo and W are mainly in their 6+ oxidation state (BE = 232.4 and 35.2 eV, respectively), niobium is present as Nb^{5+} (BE = 206.8–207.0 eV) (Table 2). Moreover, different oxidation states have been observed for vanadium and tellurium. Thus, vanadium is present as V^{5+} (BE = 517.2 eV) and V^{4+} (BE = 516.3 eV) in all samples although the V^{4+}/V^{5+} ratio decreases when increasing W/(W + Mo) ratio in the sample. By considering the surface composition of catalysts, V^{4+}/(W + Mo) and V^{5+}/(W + Mo) surface atomic ratios of 0.06 and 0.04, respectively, can be proposed for W-free sample (Table 2). However, V^{4+}/(W + Mo) and V^{5+}/(W + Mo) surface atomic ratios of 0.06 and 0.18, respectively, are obtained for Mo-free sample. Accordingly, the higher presence of V^{5+} species on the catalyst surface is favored for W-containing catalysts.

In the case of tellurium, Te^{4+} (BE = 576.2 eV) is only observed in the surface of both the Mo-free and W-free samples (Fig. 5, spectra a and d). However, Te^{4+} (BE = 576.2 eV) and Te^{6+} (BE = 577.5 eV), in addition to a small amount of Te probably in the metallic phase (BE = 573.7 eV), are clearly observed in the Mo–W bronzes (Fig. 5, spectra b and c).

It has been reported that the amount of tellurium incorporated in the framework of a TTB structure in Te-containing Mo–V–Nb–P bronzes is relatively low, while the rest of tellurium in Te-rich catalysts could favor the formation of amorphous regions in the

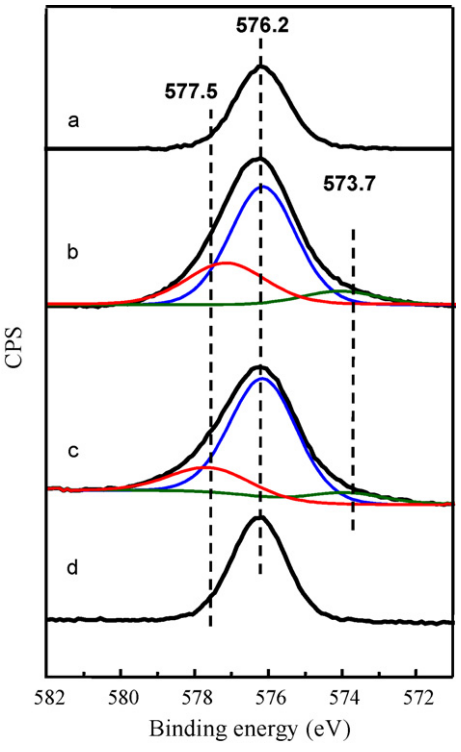

Fig. 5. X-ray photoelectron spectra corresponding of Te3d5/2: (a) MW0; (b) MW50; (c) MW75; (d) MW100.

Table 2
XPS results of Mo–W-based mixed oxides with TTB structure.

Catalyst	Mo–W–Nb–V–Te atomic ratio		Binding energy, eV				
	Bulk[a]	Surface[b]	Mo3d5/2	W4f7/2	Nb3d5/2	V2p3/2[c]	Te3d5/2[c]
MW0	1.0–0.0–0.56–0.17–0.15	1.0–0.0–0.37–0.10–0.27	232.7 eV	–	206.76 eV	516.4 eV (63.2%) 517.2 eV (36.7%)	576.5 eV
MW50	0.55–0.45–0.63–0.18–0.06	0.65–0.35–0.37–0.15–0.52	232.4 eV	35.2 eV	207.0 eV	516.3 eV (71.6%) 517.8 eV (28.3%)	577.1 eV (26.2%) 576.1 eV (64.8%) 573.9 eV (8.9%)
MW75	0.36–0.64–0.53–0.24–0.07	0.50–0.50–0.45–0.28–0.31	232.4 eV	35.2 eV	207.0 eV	516.3 eV (60.9%) 517.8 eV (39.1%)	577.1 eV (26.2%) 576.1 eV (64.8%) 573.9 eV (8.9%)
MW100	0.0–1.0–0.69–0.25–0.23	0.0–1.0–0.58–0.25–0.37	–	35.3 eV	206.8 eV	516.4 eV (26.3%) 517.4 eV (73.7%)	576.2 eV

[a] Atomic composition as determined by ICP analysis.
[b] Atomic composition as determined by XPS.
[c] In parenthesis amount of each oxidation state.

TTB crystals mainly containing tellurium and molybdenum [12]. Therefore, Te/Mo ratio of 0.02–0.04 in the synthesis gel seems to be the limit for an optimal incorporation of tellurium in framework positions. However, the effective incorporation of tellurium in Mo,W-containing catalysts could be a little different. Thus, it is clear that a greater incorporation of tellurium on the catalyst surface is favored in W-containing samples, the Mo-free catalysts being the one presenting the highest Te/Mo ratio on the surface of the catalysts.

3.2. Catalytic behavior

The catalytic performance of TTB-bronzes with different W/(W + Mo) atomic ratio and a Te/(W + Mo) atomic ratio of 0.04 has been studied in the 320–400 °C temperature range. Table 3 shows comparatively the catalytic results achieved at 380 °C. In all cases, acrolein, acrylic acid (only at high olefin conversion), carbon monoxide and carbon dioxide have been the main reaction products, although acetic acid, acetone and acetaldehyde have also been detected as minority products.

The incorporation of tungsten in the molybdate-based structure has a strong influence on their catalytic performance in olefin partial oxidation. In this sense, the W-free material (MW0) shows high selectivity to partial oxidation products (acrolein + acrylic acid, above 90%), although with low propene conversion. However, when considering the surface area of catalysts, W-free sample seems to be the most active catalyst. In fact the specific catalytic activity (in 10^4 mol_{C3} h^{-1} m^{-2}) decreases when increasing the W-content in the catalyst (Table 3). This is consistent with the fact that Mo species are involved in the selective activation of propene [29,30].

Partial substitution of molybdenum by tungsten up to W/(W + Mo) molar ratio of 0.50 favors an important increase in the propene conversion with no significant decrease of the selectivity to partial oxidation products, i.e. acrolein + acrylic acid (Fig. 6A). Nevertheless, for higher contents in tungsten, both, catalytic activity and selectivity to partial oxidation products decrease. Accordingly, the surface area of catalysts and the Mo-content on the surface of catalysts are key aspects to explain the variation of the propene conversion with the Mo/W ratio.

As can be observed in Fig. 6A the selectivity to partial oxidation products at low propene conversions is high for all MoW-catalysts especially for those rich in molybdenum. However, when increasing the conversion of propene up to 50% the selectivity hardly decreases for the Mo-rich catalysts whereas an important decrease is observed in those catalysts with the highest W-content, i.e. MW75 and MW100. Therefore it can be concluded that an excess of tungsten leads to the overoxidation of acrolein and acrylic acid to carbon oxides.

In parallel, the selectivity to acrylic acid varies also similarly with W substitution. Fig. 6B plots the variation of propene conversion and selectivity to partial oxidation products over the MW50 sample. For low propene conversion, only acrolein is produced but, for conversion values above 40% a significant quantity of acrylic acid is obtained by secondary oxidation of the aldehyde. Therefore, it is known that Mo–W–V mixed oxides, with a M_5O_{14}-like phase [5], are industrially used as catalysts for the partial oxidation of acrolein into acrylic acid.

In any case, the selectivity to acrolein + acrylic acid keeps above 85% in the whole range of conversion studied. It is also noticeable that a similar behavior has been observed by Holmberg et al. [18,19] for the ammoxidation of propene to acrylonitrile, in which partial substitution of Mo by W in the M2-phase catalyst improved its catalytic behavior in propene oxidation.

It is well known that molybdates show better catalytic performance in the olefin partial oxidation than tungstates, due to the different reducibility observed in their corresponding actives sites [31]. However, other aspects must be considered in the case of mixed oxides of both elements (Mo and W). At this point, the complexity inherent to the multicomponent system, i.e., Mo–W–Nb–V–P–Te–O makes extremely difficult to carry out a rationalization of the catalytic behavior, as already done in binary oxides [32]. It can be reasoned that the effect of W substitution is mostly structural, rather than electronic (i.e., a significant quantity of W must be introduced to produce the effect), which is in agreement with the observed XRD patterns and the reports of FTIR and Raman spectroscopy obtained for the W-containing materials. In this sense, dilution of Mo-sites in the TTB structure could result in a positive effect of site isolation [33–35]. Nevertheless, the improvement in the yield to partial oxidation products observed in the sample with atomic ratio Mo:W = 1 is much better than expected. In this case, it has been suggested that for certain range of compositions a synergic effect may be observed when Mo and W they are present in the TTB structure [10,18,19]. Moreover, as commented, the reduction of crystallite dimensions related to the incorporation of tungsten favors an increase in the catalyst surface that also favor a greater number of active sites on the catalyst surface.

Besides this, the incorporation of tellurium into the bronze framework is crucial to achieve high performance in the olefin partial oxidation [12]. Here, Te^{4+}-sites are responsible of the olefin selective activation, whereas Mo=O double bonds and, but to a lesser extent, W=O double bonds promote the O-insertion in the hydrocarbon. The role of V- and Nb-sites is still to be confirmed, although it seems to be proved that they have no direct catalytic

Table 3
Selective oxidation of propylene over Mo–W-based mixed oxides with TTB structure[a].

Sample	Conversion (%)	Selectivity (%)						Specific catalytic activity ($\times 10^4$ mol_{C3} h^{-1} m^{-2})[b]
		Acrolein	Acrylic acid	Acetaldehyde	Acetone	CO	CO_2	
MW0	22.3	91.7	1.6	1.0	2.8	1.5	1.4	2.03
MW25	34.6	86.7	2.3	1.0	2.0	4.7	3.2	1.26
MW40	35.3	70.3	10.8	1.0	2.0	10.5	5.4	1.43
MW45	37.5	78.0	8.8	0.9	1.7	6.7	3.9	1.00
MW50	62.3	79.3	10.9	0.7	1.0	5.2	2.2	1.70
MW75	53.3	44.2	9.8	0.8	0.7	31.0	13.5	1.26
MW100	36.4	65.7	2.4	0.9	1.0	22.3	7.7	0.69

[a] Reaction condition: 380 °C, $C_3^=/O_2/He/H_2O$ molar ratio of 1.5/6.0/77.5/15 and contact time, W/F, of 550 g_{cat} h $(mol_{C3})^{-1}$.
[b] Specific catalytic activity for propene conversion at 380 °C.

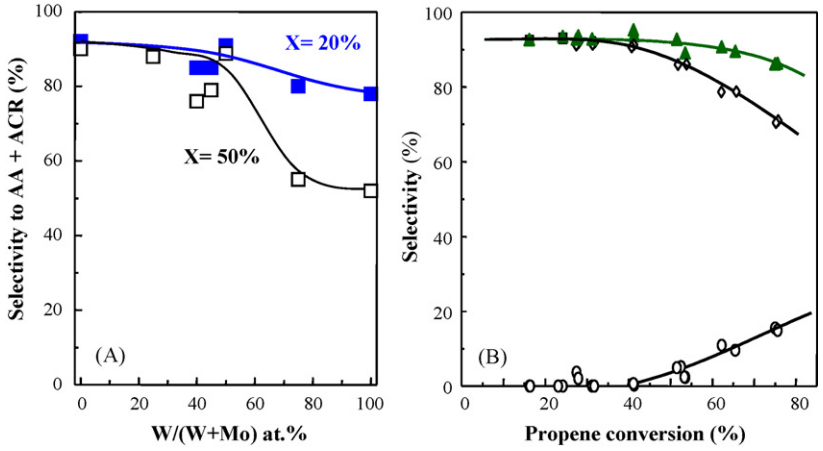

Fig. 6. Selective oxidation of propene over MoW-catalysts: (A) variation of the selectivity to partial oxidation products (i.e. acrolein and/or acrylic acid) with W/(W + Mo) ratio at a propene conversion of 20% (■) or 50% (□); (B) variation of the selective to acrolein (◊), acrylic acid (○), and the sum thereof (▲) achieved during the partial oxidation of propene over sample MW50 in the 360–400 °C reaction temperature range. Reaction conditions as in Table 3.

function in the activation of propene [18]. Therefore, it has been observed that the V/Mo and Nb/Mo surface atomic ratio increases when increasing the W-content of catalysts, while the catalytic activity shows an opposite trend.

Finally, it has been noticed that Te^{6+} in addition to Te^{4+} have been observed in samples containing both Mo and W, which show also the highest Te/Mo surface atomic ratios. Although the origin of the presence of tellurium with different oxidation state is not clear, it could be related to the formation of small islands of amorphous materials in the TTB crystals, detected in Te,Mo-containing TTB catalysts prepared with Te/Mo atomic ratio in the synthesis gels higher than 0.04, which are inactive in propene oxidation [12]. According to these results, it appears that the optimal tellurium incorporation depends also on the Mo/W ratio in the catalysts. Thus, composition must be tuned in order to improve the catalytic behavior of these catalysts.

4. Conclusions

Mo–W-containing tetragonal tungsten bronzes (TTB) can be synthesized by hydrothermal treatment of an aqueous solution of phosphomolybdic and phosphotungstic acids, vanadyl sulfate, niobium oxalate and telluric acid and further calcination of the obtained solid at 700 °C in N_2.

In the TTB structure, W can substitute Mo in the whole range up to complete replacement without the basic structure being changed. Nevertheless, due to the slightly larger Shannon ionic ratio of W^{6+}, the isomorphic substitution of Mo^{6+} by W^{6+} in the TTB framework modifies the unit cell parameters. Crystal morphology and size also vary with the incorporation of tungsten, producing slightly smaller crystallites (from 1 to 2 μm in the W-free sample to 300–400 nm in the Mo-free material).

In addition, the partial substitution of W in the Mo-containing TTB structure can modify the incorporation of the rest of elements as a consequence of the different ionic ratios and reducibility of Mo and W atoms, which can facilitate in a different way the incorporation of V^{4+}/V^{5+} and Nb^{5+}. This can also affect the incorporation of Te atoms in framework positions as concluded from the XPS results.

However, the presence of W-containing oxoanions in the synthesis gels seems to be beneficial for the textural properties of these materials, favoring the achievement of higher surface areas. In any case, Mo-sites seem to be directly involved in the activation of propene, while W-sites are less active. Moreover, an systematic study on the influence of catalyst composition on catalytic behavior needs to be carried out in order to improve the formation of acrolein and acrylic acid.

Acknowledgements

Financial support from DGICYT in Spain through Projects CTQ2006-09358/BQU, is gratefully acknowledged. Authors are also grateful to Manuel Planes Insausti and Jose Luis Moya López, technical supervisors responsible for the Servicio de Microscopía Electrónica (UPV) for the use of their facilities.

References

[1] A. Mágneli, Ark. Kemi 1 (1949) 269.
[2] C.N.R. Rao, Pure Appl. Chem. 66 (1994) 1765.
[3] U.B. Mioc, R.Z. Dimitrijevic, M. Davidovic, Z.P. Mitrovic, Ph. Colomban, J. Mater. Sci. 29 (1994) 3705.

[4] R.Z. Dimitrijevic, Ph. Colomban, U.B. Mioc, Z. Cedic, M.R. Todorovic, N. Tjapkin, M. Davidovic, Solid State Ionics 77 (1995) 250.
[5] G. Mestl, T. Ilkenhans, D. Spielbauer, M. Dieterle, O. Timpe, H.J. Krohnert, F. Jentoff, H. Knözinger, R. Schlögl, Appl. Catal. A: Gen. 210 (2001) 13.
[6] K. Wasserman, M.T. Pope, M. Salmen, J.N. Dann, H.-J. Lunk, J. Solid State Chem. 149 (2000) 378.
[7] (a) W. Ueda, N.F. Chen, K. Oshihara, Chem. Commun. (1999) 517;
(b) D. Vitry, Y. Morikawa, J.L. Dubois, W. Ueda, Appl. Catal. A: Gen. 251 (2003) 411.
[8] H. Watanabe, Y. Koyasu, Appl. Catal. A: Gen. 194–195 (2000) 479.
[9] (a) P. Botella, J.M. López Nieto, A. Martínez-Arias, B. Solsona, Catal. Lett. 74 (2001) 149;
(b) P. Botella, E. García-González, J.M. López Nieto, J. González-Calbet, Solid State Sci. 7 (2005) 507.
[10] P. Botella, B. Solsona, E. García-González, J.M. González-Calbet, J.M. López Nieto, Chem. Commun. (2007) 5040.
[11] P. Botella, B. Solsona, J.M. López Nieto, Catal. Today 141 (2009) 311.
[12] P. Botella, E. García-González, B. Solsona, E. Rodríguez-Castellón, J.M. González-Calbet, J.M. López Nieto, J. Catal. 265 (2009) 43.
[13] J. Rodríguez-Carvajal, FullProf, version 3.30, Laboratoire Léon Brillouin (LLB), 2005.
[14] Lundberg, M. Sundberg, A. Mágneli, J. Solid State Chem. 44 (1982) 32.
[15] B.O. Marinder, Angew. Chem. Int. Ed. 25 (1986) 431.
[16] R.D. Shannon, Acta Crystallogr. Sect. A 32 (1976) 751.
[17] A.R. Denton, N.W. Ashcroft, Phys. Rev. A 43 (1991) 3161.
[18] J. Holmberg, S. Hansen, R.K. Grasselli, A. Andersson, Top. Catal. 38 (2006) 17.
[19] J. Holmberg, J.B. Wagner, R. Häggblad, S. Hansen, L.R. Wallenberg, A. Andersson, Catal. Today 128 (2007) 153.
[20] P. Botella, J.M. López Nieto, B. Solsona, Catal. Lett. 78 (2002) 383.
[21] P. Afanasiev, J. Phys. Chem. B 109 (2005) 18293.
[22] G. Harley, K.D. Krever, J. Maier, L.G. de Jonghe, J. Non-Cryst. Sol. 355 (2009) 932.
[23] M. Scheithauer, R.K. Grasselli, H. Knözinger, Langmuir 14 (1998) 3019.
[24] W.L. Liu, H.R. Xia, X.Q. Wang, H. Han, G.W. Lu, Mater. Chem. Phys. 90 (2005) 134.
[25] S. Xie, K. Chen, A.T. Bell, E. Iglesia, J. Phys. Chem. B 104 (2000) 10059.
[26] J.M. Amarilla, M.L. Pérez-Revenga, B. Casal, E. Ruiz-Hitsky, Catal. Today 78 (2003) 571.
[27] G. Deo, I.E. Wachs, J. Phys. Chem. 95 (1991) 5889.
[28] F.D. Hardcastlet, I.E. Wachs, J. Phys. Chem. 95 (1991) 5031.
[29] R.K. Grasselli, J.D. Burrington, D.J. Buttrey, P. DeSanto Jr., C.G. Lugmair, A.F. Volpe Jr., T. Weingand, Top. Catal. 23 (2003) 55.
[30] J. Holmberg, R.K. Grasselli, A. Andersson, Appl. Catal. A: Gen. 270 (2004) 121.
[31] R.K. Grasselli, in: G. Ertl, H. Knözinger, J. Weitkamp (Eds.), Handbook of Heterogeneous Catalysis, Wiley–VCH, New York, 1997, pp. 2302–2326.
[32] (a) G. Centi, F. Trifiró, Appl. Catal. 12 (1984) 1;
(b) P.L. Villa, G. Caputo, F. Sala, F. Trifiró, J. Catal. 31 (1973) 200.
[33] F. Smet, P. Ruiz, B. Delmon, M. Devillers, J. Phys. Chem. B 105 (2001) 12355.
[34] J.L. Callahan, R.K. Grasselli, AIChE J. 9 (1963) 755.
[35] R.K. Grasselli, Top. Catal. 15 (2001) 93.